Geophys. J. Int. (2000) **141,** 672–678

On the microseisms associated with coastal sea waves

Ezekiel O. Okeke and Vincent E. Asor*

Department of Mathematics, University of Benin, Benin City, Nigeria. E-mail: v.e.asor@openmail2.dtw-itp.spdcwri.simis.com

Accepted 2000 January 4. Received 2000 January 4; in original form 1998 June 16

SUMMARY

We present a model that concerns microseisms in the period range between 7 and 9 s. In this modelling we have incorporated the effects of incident and reflected sea waves along the shoreline. A relationship between the phenomena of wave reflection along the shoreline and microseisms is suggested by this study. In addition, the far-field microseismic energy computed from this model is considerably larger than our two previous calculations (Darbyshire & Okeke 1969; Okeke 1972) and, interestingly, closer to that obtained from recent measurements (Trevorrow *et al.* 1989). A possible explanation is that the present model incorporates the activity of the wave train approaching the shoreline from a wide range of directions. Thus, it is a generalization of the normal incident theory originally proposed by Darbyshire & Okeke (1969) and employed in our two previous calculations (Darbyshire & Okeke 1969; Okeke 1972).

This model also estimates the distance from the shoreline over which the approaching shallow water waves are expected to acquire measurable bottom pressure and confirms that this distance is proportional to the wave period (Fig. 3).

Furthermore, by assuming that the elastic parameters in the far field are functions of the vertical coordinate only, the depth dependence of frequency bandwidth and the associated spectral energy peak are calculated. The results depict reasonably well the possible effects of structural layering below the Earth's surface in the locality.

Key words: coastal sea waves, microseisms.

1 INTRODUCTION

The small-scale earth tremors known as microseisms are vibrations of the solid earth with an amplitude of about 10 μm. These vibrations usually appear on earthquake records. However, they are usually regarded as a nuisance by seismologists because they tend to distort the earthquake records. Nevertheless, their appearance on seismographs usually heralds approaching storms. Therefore, one of their major uses is in weather forecasting, and recently, but more importantly, they have proved useful in geophysical inverse problems (Trevorrow & Yamamoto 1991).

The coupling of microseismic energy with that of sea waves has long been established. Two frequency bands are identifiable: these are the double-frequency band (Longuet-Higgins 1950; Hasselmann 1963; Darbyshire & Okeke 1969; Kibblewhite & Ewans 1985) and the single-frequency band (Darbyshire & Okeke 1969; Okeke 1972; Goodman *et al.* 1989; Trevorrow *et al.* 1989). The various mechanisms for the excitation of the two bands have also been established quantitatively.

However, there is still what may be regarded as the intermediate frequency band, which lies between the double- and the single-frequency bands. It ranges from approximately 7 to 9 s period and is consistently present in analysed wave records. In this range, there is no relationship identical to that of single- or double-frequency microseisms within the band; that is, within this frequency band the peak energy densities of the microseisms lie neither at the same frequency nor at twice the frequency of the current-generating water waves (Darbyshire & Okeke 1969). This work is therefore concerned with the modelling of microseisms that have periods in the range 7–9 s.

We attempt to estimate the energy of microseisms and that of the related sea waves arising from interaction with the coast. In previous attempts, Darbyshire & Okeke (1969) assumed a model of normal incidence and reflected waves on a rocky coastline. Okeke (1972, 1985) improved on this by assuming that the angle of incidence ranges from 0 to $\pi/2$. However, the reflected wave energy was neglected in the computation. An attempt will now be made to generalize these two successful models and use them to study the generation of microseisms in the range of intermediate frequencies.

2 THE WAVENUMBER SPECTRUM FOR COASTAL REFLECTED WAVES

The technique developed by Darbyshire & Okeke (1969) will be exploited and further generalized. The subscripts i and r refer to incident and reflected wave components, respectively, along the coastline. Let $\Delta K = K_i - K_r$ be the wavenumber

* Present address: The Shell Petroleum Development Company of Nigeria Limited, Warri, Nigeria.

difference. We now divide ΔK into n subdivisions each of width δK_p, thus $\Delta K = n\delta K_p$. With fixed frequency ω, $C_m = \omega/K_m$, where C_m and K_m are the phase velocity and wavenumber, respectively, in the range of high-phase velocity pressure components.

For the incident modes, the spectral amplitudes for the subdivisions are $h_1, h_2, \ldots, h_n$, and for the reflected modes, $g_1, g_2, \ldots, g_n$. Here, $h_i = h_i(R, \omega, K_i, \theta_i)$, $g_r = g_r(R, \omega, K_r, \theta_r)$; these functions contain the angles of incidence and reflection, which will generally be equal. The resultant spectral amplitude is obtained by the convolution of the two; that is,

$$\sum_{r=1}^{n} \sum_{i=1}^{n} g_r h_i \delta_{ri},$$

where $\delta_{ri} = 1$ when $r = i$ and $\delta_{ri} = 0$ when $r \neq i$; δ_{ri} is the Kronecker delta. Consequently, $r = i$ corresponds to the case of constructive interference and $r \neq i$ to that of destructive interference.

Now, $g_r = h_i R_f$, $i = r$, where R_f is a reflection coefficient. Thus, for $r = i$,

$$\sum_{i=1}^{n} g_i h_i = \sum_{i=1}^{n} g_i^2 R_f$$

and $\bar{\theta}$ representing the mean value of θ_r, we obtain

$$\sum_{i=1}^{n} R_f g_i^2 = R_f S_1(\omega, K_0, \bar{\theta}) n \delta K_p, \qquad K_0 \gg K_m, \tag{2.1}$$

where K_0 is the wavenumber of the gravity mode and $S_1(\omega, K_0, \bar{\theta})$ represents the spectral amplitude.

To a reasonable degree of accuracy, the power spectrum of a system is proportional to the square of the amplitude spectrum. Thus, for $-\infty < K_0 < \infty$,

$$S_p(K_0, \omega, \bar{\theta}) = R_f S_1^2(K_0, \omega, \bar{\theta}) n \delta K_p, \tag{2.2}$$

where $S_p(K_0, \omega, \bar{\theta})$ is the power spectrum of the sea wave. The inequality immediately before eq. (2.2) implies that both high and low phase velocity wavenumber components arising from the linear modulation of the gravity (water) wave bottom pressure are now involved (Hasselmann 1963).

3 DETERMINATION OF THE SEA-WAVE POWER SPECTRUM.

In this model, an oscillatory wave train approaching a shoreline at an angle $\bar{\theta}$ is considered. Here, $\bar{\theta}$ is measured from the line normal to the shoreline. The sea bottom is uniformly sloping with a gradient α but is not necessarily parallel to the shoreline. Then, following Okeke (1972, 1985), the wave bottom pressure in this study takes the usual form,

$$P_{33} = \rho_w g \sqrt{\frac{d}{R}} J_0\left(2\omega\sqrt{\alpha\frac{R}{g}}\right) \cos\frac{\bar{\theta}}{2} \cos\omega t, \qquad 0 < \bar{\theta} < \frac{\pi}{2}, \tag{3.1}$$

where ρ_w is the water density, R is the radial distance, d is the width of the shelf, which includes the breaking zone, as measured from the shoreline, J_0 is a zero-order Bessel function of the first kind and g represents the acceleration due to gravity.

The components of the Fourier–Bessel coefficients corresponding to eq. (3.1) are

$$CH(K, \bar{\theta}, \omega) = \frac{\alpha d^{-1/2}}{(K_0 + K_m)^{1/2}} J_0\left[\frac{\omega^2 \alpha g^{-1}}{K_0 + K_m}\right] \cos\frac{\bar{\theta}}{2} \tag{3.2}$$

and

$$SH(K, \bar{\theta}, \omega) = \frac{\alpha d^{-1/2}}{(K_0 - K_m)^{1/2}} J_0\left[\frac{\omega^2 \alpha g^{-1}}{K_0 - K_m}\right] \cos\frac{\bar{\theta}}{2}. \tag{3.3}$$

Eqs (3.2) and (3.3) give the spectral amplitudes in the K_0-plane for the linear bottom pressure of the gravity wave in shallow water.

In the range of very low frequencies considered here,

$$J_0\left[\frac{\omega^2 \alpha g^{-1}}{K_0 + K_m}\right] \to J_0\left[\frac{\omega^2 \alpha g^{-1}}{K_0 - K_m}\right] \to 1. \tag{3.4}$$

The approximation in eq. (3.4) was utilized in the calculations involving the range of primary frequency microseisms. However, in the intermediate range, the whole expressions in eqs (3.2) and (3.3) will be used in the computations; note that $K \gg K_m$. Thus, with a 1 per cent variation in the wavenumber, the amplitude spectral density is defined by

$$\begin{aligned} S_1^2(K_0, \omega, \bar{\theta}) &= [CH^2(K_0, \omega) + SH^2(K_0, \omega)] \\ &= \frac{2\alpha^2 d^{-1}}{K_0} J_0^2\left[\frac{\omega \alpha g^{-1}}{K_0}\right] \cos^2\frac{\bar{\theta}}{2}. \end{aligned} \tag{3.5}$$

Eq. (3.5) suggests that the spectral density favours a long but finite breaker zone and a rather gently sloping beach. It gives the power of the pressure wave per unit wavenumber in the water layer. This conclusion is quantitatively in agreement with the observed behaviour of microseisms and the generation of sea waves.

4 SEISMIC RESPONSE

Although this paper is an extension of the previous papers, it may be instructive to recapitulate the basic equations governing the processes of stress waves in an elastic and homogeneous half-space. The components of the ground displacement in response to the passage of seismic oscillations are usually given by

$$U_R = \frac{\partial\phi}{\partial R} + \frac{\partial^2\psi}{\partial R\partial z}, \tag{4.1}$$

$$U_z = \frac{\partial\phi}{\partial z} - \frac{\partial^2\psi}{\partial R^2} - \frac{\partial\psi}{R\partial R}, \tag{4.2}$$

where U_R is the radial component of displacement, U_z is the vertical component of displacement, ϕ and ψ are potential functions associated with the compressional wave with speed α_0 and the shear wave with speed β_0, respectively, z is the vertical coordinate measured from the seabed downwards and R is the radial distance.

If we write $\phi = \mathscr{Re}[\phi_0(R, z)\,e^{i\omega t}]$ and $\psi = \mathscr{Re}[\psi_0(R, z)\,e^{i\omega t}]$, then ϕ_0 and ψ_0 satisfy the equations

$$\left(\frac{\partial^2}{\partial R^2} + \frac{\partial}{R\partial R} + \frac{\partial^2}{\partial z^2} + \frac{\omega^2}{\alpha_0^2}\right)\phi_0 = 0, \tag{4.3}$$

$$\left(\frac{\partial^2}{\partial R^2} + \frac{\partial}{R\partial R} + \frac{\partial^2}{\partial z^2} + \frac{\omega^2}{\beta_0^2}\right)\psi_0 = 0, \tag{4.4}$$

where

$$K^2 = K_{\alpha_0}^2 + \frac{\omega^2}{\alpha_0^2} = K_{\beta_0}^2 + \frac{\omega^2}{\beta_0^2}. \tag{4.5}$$

The formal integral representations of the solutions of eqs (4.3) and (4.4) using eq. (4.5) are, respectively,

$$\phi_0 = \int_0^{\infty} A(K) J_0(KR) K \exp(-K_{\alpha_0} z)\, dK \tag{4.6}$$

and

$$\psi_0 = \int_0^{\infty} B(K) J_0(KR) K \exp(-K_{\beta_0} z)\, dK\,. \tag{4.7}$$

In this study, we are concerned with the vertical displacement. This can be derived from eqs (4.6) and (4.7) as follows:

$$U_z(R, z, t) = \mathscr{Re}\left[\mathrm{e}^{-i\omega t} \int_0^{\infty} K^2 (K_{\alpha_0} A(K) \exp(-K_{\alpha_0} z) + K^2 B(K) \exp(-K_{\beta_0} z)) J_0(KR)\, dK \right]. \tag{4.8}$$

In eq. (4.8) the spectral amplitudes $A(K)$ and $B(K)$ are calculated from the following boundary conditions at $z = 0$.

(1) Vanishing of tangential stress, which gives

$$2K_{\alpha_0} A(K) - \left(2K^2 - \frac{\omega^2}{\beta_0^2}\right) B(K) = 0\,. \tag{4.9}$$

(2) The vertical stress component has to be balanced by the high phase velocity random pressure components that are associated with the propagating gravity water waves, i.e.

$$\left(\lambda + \rho_s \lambda' \frac{\partial}{\partial t}\right) \nabla^2 \phi + 2\left(\mu + \rho_s \mu' \frac{\partial}{\partial t}\right) \frac{\partial U_z}{\partial z} = \int_0^{\infty} K P_{33} J_0(KR_0)\, \mathrm{e}^{i\omega t}\, dK\,, \tag{4.10}$$

where $P_{33} = P_{33}(\omega, \bar{\theta}, R, t)$ is defined in eq. (3.1), λ and μ are elastic constants and λ' and μ' are the corresponding parameters associated with damping in the solid earth with density ρ_s.

Solving eqs (4.9) and (4.10),

$$B(K, \omega) = 2K_{\alpha_0} \frac{P_{33}}{\rho_s \Delta(K, \omega)}\,,$$

$$A(K, \omega) = \frac{\left(2K^2 - \frac{\omega^2}{\beta_0^2}\right) P_{33}}{\rho_s \Delta(K, \omega)}\,,$$

where

$$\Delta(K, \omega) = (\beta_0^2 + i\omega\lambda') \left[\left(2K^2 - \frac{\omega^2}{\alpha_0^2}\right)\left(2K^2 - \frac{\omega^2}{\beta_0^2}\right) - 4K^2 K_{\alpha_0} K_{\beta_0} \right] \tag{4.11}$$

is the Rayleigh function (Bullen & Bolt 1985).

Assume that

$$F(K, \omega) = \left(\frac{\beta_0}{\omega}\right)^2 \Delta(K, \omega)\,. \tag{4.12}$$

$F(K, \omega)$ is also the Rayleigh function but multiplied by a factor of $(\beta_0/\omega)^2$ This factor drops out in the subsequent calculations involving the function, except in the essential computations of $\delta\omega(z)$.

5 DETERMINATION OF THE SPECTRAL WIDTH

Moving nearer to deep-water areas, where linear bottom pressure vanishes, we have

$$F(K, \omega) = F(K', \omega) + \delta K \frac{\partial F}{\partial K}(K, \omega)|_{K=K'} + (\delta K)^2 = 0\,, \tag{5.1}$$

from which

$$\delta K = \frac{-F(K', \omega)}{\partial F / \partial K(K', \omega)}\,, \tag{5.2}$$

where K' is the value of K for which eq. (5.1) is satisfied and

$$\frac{\partial F}{\partial K} = \frac{C_m}{K_m} \frac{\partial F}{\partial V}\,, \tag{5.3}$$

with $C_m = 2.8$ km s^{-1} and $\partial F / \partial K = 65.3 \partial F / \partial V$ (km, s units), where V is the group velocity for the seismic modes.

Numerical evaluation of eqs (5.2) and (5.3) when $K' = 0.30$ km^{-1} (wavelength of about 20.9 km) gives

$$\delta K = 3.1 \times 10^{-4}\ \mathrm{km}^{-1}\,. \tag{5.4}$$

The result in eq. (5.4) suggests that the spectrum for the elastic solid is as expected; that is, it is highly peaked. Thus, the dominant mode is associated with a far greater proportion of elastic wave energy.

However, the wave energy or amplitude spectrum is usually calculated in terms of frequencies rather than wavenumbers. Thus, following the same procedure adopted in deriving eq. (5.2), the frequency bandwidth is given by

$$\delta\omega = \left(\frac{4\pi^2 \beta_0^2}{\lambda_m^2 \omega_m}\right)\left(\frac{96 - 128\alpha_1^2 + 16\alpha_1^4 - \alpha_1^6}{256 - 64\alpha_1^2 + 6\alpha_1^4}\right), \quad \delta f = \delta\omega / 2\pi\,, \quad \alpha_1 = c/\beta_0 < 1\,, \tag{5.5}$$

where λ_m and μ_m are the wavelength and frequency associated with the dominant mode in the vibration of the elastic medium.

First, we note the strong dependence of $\delta\omega$ on β_0. Consider the case of a stratified medium in which β_0 is a function of the vertical coordinate below the Earth's surface ($\beta_0 = \beta_0(z)$). Thus, $\delta\omega = \delta\omega(z)$. Furthermore, in spite of the factor β_0^2 on the right-hand side of eq. (5.5), $\delta\omega(z) \ll 1$. The inequality applies at all depths below the Earth's surface over which microseismic signals are detectable. This statement is confirmed by numerical calculations, using the shear velocity vertical profile extrapolated from the reference shear wave velocity profile as the data source (Bullen & Bolt 1985; Yamamoto & Torri 1986; Trevorrow & Yamamoto 1991) (Fig. 1). This compares well with the records from our local data source. The computed values of δf as a function of z are shown in Fig. 2. If we assume that $z = 1.1$ m and the period is 8 s, then $(\delta\omega)^2 = 16.9 \times 10^{-8}$(rad s^{-1})^2. These data are those frequently used for theoretical calculations involving the peak energy of the solid ground vertical displacement. Thus, $z = 1.1$ m suggests the likely depth of burial of a land-based seismometer. Calculations from eq. (5.5) further verify that $\delta\omega$ is a decreasing function of β_0. Fig. 1 depicts the form of the vertical structures of the elastic medium to a depth of about 100 m below the Earth's surface in the locality (Trevorrow *et al.* 1989).

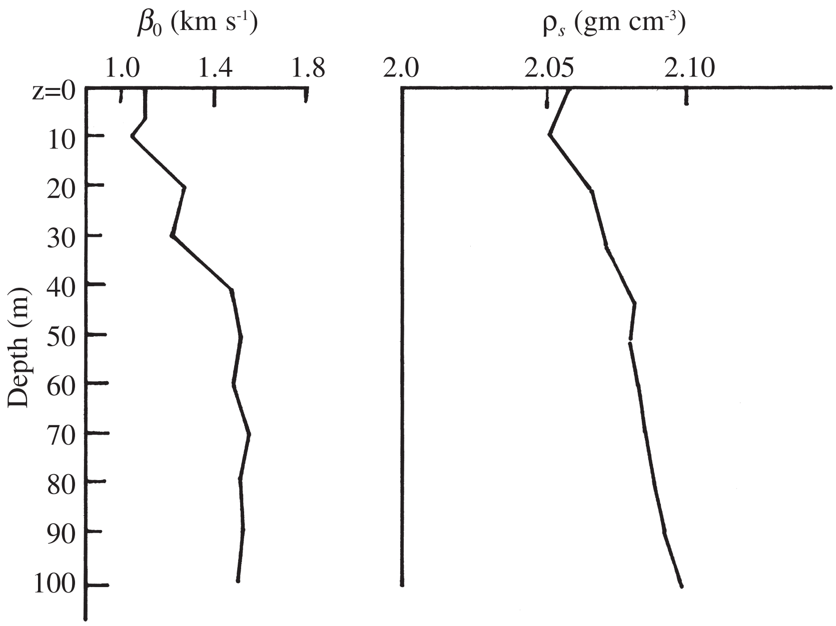

Figure 1. The variation of β_0 and ρ_s with depth for far-field shallow seismic structures.

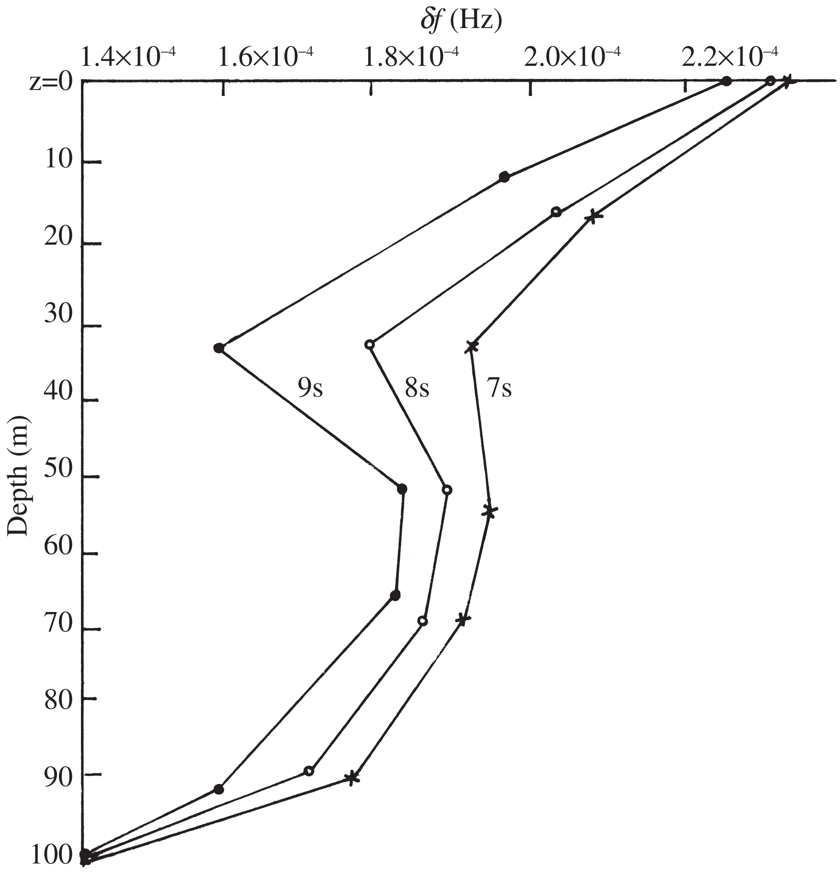

Figure 2. Variation of frequency bandwidth with depth below the Earth's surface for seismic waves of periods 7, 8 and 9 s.

6 TRANSFER FUNCTION

$\mu' = \gamma\alpha_0^{-2}$ and $\lambda' = \gamma\beta_0^{-2}$, where γ is the damping coefficient (Okeke 1972). Eventually, eq. (4.8) takes the form

$$U_z(R, \omega)\,e^{-0.11\gamma t} = 2\int_0^{\infty}\left[\frac{KJ_0(KR_0)P_{33}(K, \omega, \theta)}{\rho_s F(K, \omega)}\right]dk\,. \qquad (6.1)$$

For large R, we use the asymptotic form of $J_0(KR)$, thus

$$J_0(KR) = \left(\frac{2}{\pi KR}\right)^{1/2}\cos\left(KR - \frac{\pi}{4}\right), \qquad (6.2)$$

$K = K(K_0, K_p)$, $20\ \mathrm{km}^{-1} \le K_0 \le 100\ \mathrm{km}^{-1}$, $0.1\ \mathrm{km}^{-1} \le K_p \le 0.4\ \mathrm{km}^{-1}$. Applying the stationary phase method to the evaluation of eq. (6.1) using eq. (6.2),

$$U_z(R, \omega)\,e^{-0.11\gamma t} = \frac{2P_{33}(K_0, \omega)}{\rho_s}\left(\frac{2}{\pi R}\right)^{1/2}\sum_K\left(\frac{\sqrt{K}}{\partial F/\partial K}\right)\delta(K - K_p), \qquad (6.3)$$

where $\delta(K - K_p)$ is the delta function. $\sum_K$ implies that the summation is over all possible values of K in the spectrum. However, the contribution to eq. (6.3) will come from those values of K that are the roots of $F(K, \omega) = 0$.

We now evaluate the amplitude spectrum in the K-plane for the left- and right-hand sides of eq. (6.3). The convolution theorem is used to evaluate the power associated with the product on the right-hand side. Thus, in terms of the amplitude spectrum,

$$S_u(K, \omega, \bar{\theta}) = S_p(K_0, \omega, \bar{\theta})H(K_p, \omega), \qquad (6.4)$$

where $H(K_p)$ is the amplitude spectrum for the function

$$\left(\frac{2}{\pi R}\right)^{1/2}\sum_K\left[\left(\frac{\sqrt{K}}{\partial F/\partial K}\right)\delta(K - K_p)\right]. \qquad (6.5)$$

Using the sampling property of the delta function, the spectral energy density becomes

$$H^2(K_p, \omega) = \left[\frac{2K}{\pi R}\left(\frac{\partial F}{\partial K}\right)^{-2}\right]_{K=K_p}. \qquad (6.6)$$

The spectrum expressed by eq. (6.6) is strongly peaked when $K_p = K_m$; δK is the width of the spectrum. However, due to the damping factor, the spectral peak height is still finite and a function of R.

7 ESTIMATE OF THE SHELF WIDTH

We take $\Delta\omega$ as the angular frequency difference between two successive maxima in the spectra of the incident and reflected beach waves. Using some of the relations for the shallow water waves, the characteristic linear wave speed $c_0 = \sqrt{(gh_0)}$, h_0 being the depth of the water layer measured from the undisturbed free surface, and $\omega^2 = K_0^2 C_0^2$. Thus, $\Delta K_0 = \Delta\omega/\sqrt{(gh_0)} = 0.0081K_0 = 0.051/L_0$; ΔK_0 is the change in K_0 between two successive maxima in the wavenumber spectrum and L_0 is the corresponding wavelength ($L_0 = 2\pi/K_0$).

With $\omega = 2\pi i$, where $f = 0.11$ Hz, $C_0 = 15\ \mathrm{m\ s}^{-1}$, $h_0 = 22$ m and $\Delta K_0 = 1.4 \times 10^{-4}\ \mathrm{km}^{-1}$, $d = 0.002\pi/\Delta K_0$. This relationship suggests that d is an increasing function of the wave period (Fig. 3). If the wave period is 8 s then $d = 45$ km. This value agrees with that obtained by computing the orthogonal spacing, the corresponding group velocity V_g and hence the wave bottom pressure. The data are from a refraction diagram for an 8 s water wave (Darbyshire & Okeke 1969; Kinsman 1965). In this case, d is the distance from the shoreline (seawards), where the wave bottom pressure is appreciable enough to contribute significantly to the generation of microseisms in the shallow-water zone.

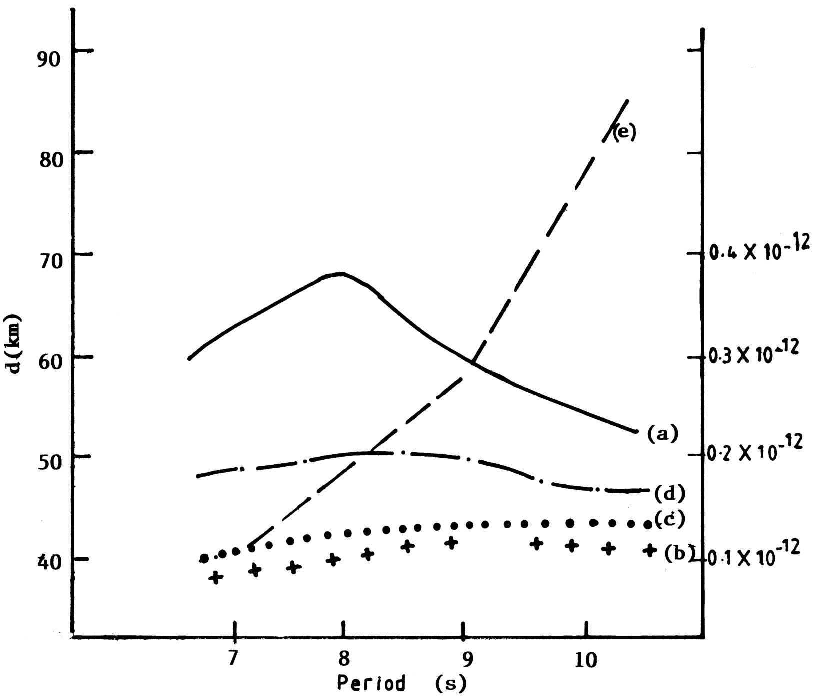

Figure 3. The ratio of the energy spectrum of microseisms and sea waves as a function of wave period. (a) Observed values Darbyshire & Okeke (1969); (b) theoretical calculations Darbyshire & Okeke (1969); (c) theoretical calculations Okeke (1972); (d) theoretical calculations (this paper); (e) variation of shelf width with wave period.

8 DISCUSSION

The relative energies of microseisms and associated sea waves are computed from eq. (6.4). R is now assigned a value of 13 km. This represents the average distance of a seismometer on the land measured from the ocean bottom seismic source near the coastline. In previous calculations, R_f was taken to be 1/30, corresponding to the value found by Savarensky and colleagues for Lake Yussi-Kul (Darbyshire & Okeke 1969). In their investigation, the coastline was assumed to be rocky. However, calculations based on wave reflection theory (Jackson 1962) gave a mean value of $R_f = 1/38$. This value allows for the finite angle of incidence and reflection, thus it seems more realistic.

The calculations from this study are displayed in Fig. 3(d) together with the following.

(a) Those computed from the simultaneous records of microseisms and sea waves. These records were from the sea wave and microseism database collected from Rhosneigr and the Menai Bridge, Anglesey. The data previously reported in Darbyshire & Okeke (1969) originated from the same source.

(b) Those computed using the normal incident theory of Darbyshire & Okeke (1969) from their eq. (4.23).

(c) Those computed from eq. (44) of Okeke (1972).

On the whole, the present model represents an improvement over our two previous investigations. Furthermore, Fig. 3(d) gives results that are comparable with those from more recent analyses (Trevorrow *et al.* 1989), thus suggesting that the phenomenon of wave reflection along coastlines contributes significantly to the spectral distortions observed in the intermediate frequency range of the spectrum. However, it should be noted that the data and subsequent calculations in Fig. 3 were based on far-field microseismic events. Those of Trevorrow *et al.* (1989) were from seafloor microseismic records. Although fairly similar, the two studies were based on two different Earth structures.

Finally, this theoretical modelling concerned the problem of the microseismic wavefield generated by the activities of random pressure waves acting on the fluid/solid interface. The microseisms originating from this process propagate to the far-field recording station in the form of guided elastic surface waves as expressed by eq. (4.8). Along this guide, it is assumed that the mean elastic parameters are generally constant. However, any slight variation associated with these is reasonably well accounted for by the introduction of damping factors in the governing equations for the elastic modes.

In addition, the denominators each eqs (6.1) and (6.6) contain $\rho_s(z)$ and $\beta_0(z)$, hence the energy ratio of microseismic and gravity waves will depend on the depth below the Earth's surface. Thus, we now divide the region below the Earth's surface into 20 parallel subdivisions. These are given by $z = 1.2, 5, 10, \ldots, 100$ m. Using the vertical Earth structure given in Fig. 1 as input data and the finite difference method, the calculations that resulted in the energy ratio shown Fig. 3(d) are repeated at each subdivision for the specified wave periods. The calculations were simplified by the replacement of the quantity $\partial F/\partial V$ in eq. (5.3) by $(\partial F/\partial z)/(\partial V/\partial z)$ and the assumption that the layer between two subdivisions is homogeneous.

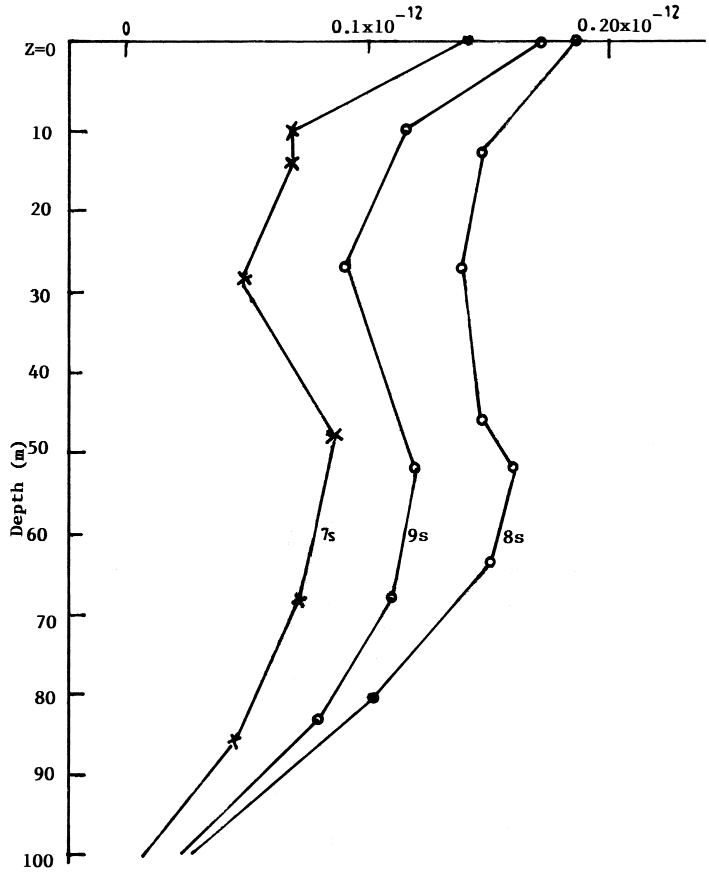

Figure 4. Vertical profiles of the energy ratio for waves of periods 7, 8 and 9 s.

The results are shown in Fig. 4. From this figure, the layers with low shear strength generally corresponds to those with high energy ratio. The energy ratios are thus apparently a decreasing function of the depth below the Earth's surface. The decrease is more rapid at depths below 70 m. Our calculations further suggests that the energy ratio is vanishingly small at depths of about 100 m and below.

We also note that because of the presence of $\rho_s(z)$ in the denominator of the energy density ratio, the depth variation of the latter does not closely follow that of the spectral bandwidth in Fig. 2.

9 CONCLUSIONS

Usually, appreciable microseisms are generated by the high phase velocity components of seafloor pressure fluctuations caused by water waves. There is no doubt that these components will possess sufficient energy to resonate the seismic modes within the seabed effectively considering the intense wave activity that frequently dominates shallow-water areas. Eq. (6.4) governs this process, with $S_p(K_0, \omega, \bar{\theta})$ as the functional representation of the water wave amplitude spectrum. This spectrum is derived from linear shallow water theory and hence has been used effectively in the study of single-frequency microseisms and those at intermediate frequency ranges.

On the other hand, the double-frequency microseisms are excited through second-order effects associated with sea waves. The amplitude spectrum of bottom pressure in this case must incorporate in its structure the activities of waves with equal and opposite wavenumbers. Thus, to apply the results derived from the present study to the double-frequency band, one only needs to formulate a different form of $S_p(K_0, \omega, \bar{\theta})$ from the solution obtained from the interacting sea waves.

ACKNOWLEDGMENTS

We are indebted to the Editor and the referees for their comments, which have greatly improved the original version of this paper. A large volume of material used in the review stage was obtained from Mark Trevorrow and we are very grateful for his assistance.

REFERENCES

Bullen, K.E. & Bolt, B.A., 1985. *An Introduction to the Theory of Seismology,* 4th edn, Cambridge University Press, London.

Darbyshire, J. & Okeke, E.O., 1969. A study of primary and secondary microseisms recorded in Anglesey, *Geophys. J. R. astr. Soc.,* **17,** 63–92.

Goodman, D., Yamamoto, T., Trevorrow, M., Abbott. C., Target, A., Badly, M. & Ando, K., 1989. Direction spectra observations of seafloor microseisms from an ocean bottom seismometer array, *J. acoust. Soc. Am.,* **86,** 2309–2317.

Hasselmann, K., 1963. A statistical analysis of the generation of microseisms, *Rev. Geophys.,* **1,** 177–210.

Jackson, J.D., 1962. *Classical Electrodynamics,* John Wiley, New York.

Kibblewhite, A.C. & Ewans, K.C., 1985. Wave–wave interactions, microseisms and infrasonic ambient noise in the ocean, *J. acoust. Soc. Am.,* **78,** 981–995.

Kinsman, B., 1965. *Wind Waves,* Prentice Hall, Englewood Cliffs, NJ.

Longuet-Higgins, M.S., 1950. A theory of the origin of microseisms, *Phil. Trans. R. Soc. Lond.,* **27,** 289–299.

Okeke, E.O., 1972. A theoretical model of primary frequency microseisms, *Geophys. J. R. astr. Soc.,* **27,** 289–299.

Okeke, E.O., 1985. On the characteristic damping of microseisms in shallow water, *Bol, Geof. Teor. Appl.,* **xxvii,** 239–242.

Trevorrow, M. & Yamamoto, T., 1991. Summary of marine sedimentary shear modulus and acoustic speed profile results using a gravity wave inversion technique *J. acoust. Soc. Am.,* **90,** 441–456.

Trevorrow, M., Yamamoto, T., Turgut, A. & Goodman, D., 1989. Measurements of ambient seabed seismic levels below 1.0Hz on shallow water Eastern US continental shelf, *J. acoust. Soc. Am.,* **86,** 2318–2327.

Yamamoto, T. & Torri, T., 1986. Seabed shear modulus profile inversion using surface gravity wave induced bottom motion, *Geophys. J. R. astr. Soc.,* **85,** 413–431.